MCB
Journals.ASM.org

USP17- and SCF$^{\beta TrCP}$-Regulated Degradation of DEC1 Controls the DNA Damage Response

Jihoon Kim,[a] Sara D'Annibale,[a] Roberto Magliozzi,[a] Teck Yew Low,[b,c] Petra Jansen,[a] Indra A. Shaltiel,[d] Shabaz Mohammed,[b,c] Albert J. R. Heck,[b,c] Rene H. Medema,[d] Daniele Guardavaccaro[a]

Hubrecht Institute-KNAW and University Medical Center Utrecht, Utrecht, The Netherlands[a]; Biomolecular Mass Spectrometry and Proteomics, Bijvoet Center for Biomolecular Research and Utrecht Institute for Pharmaceutical Sciences, Utrecht University, Utrecht, The Netherlands[b]; The Netherlands Proteomics Center, Utrecht, The Netherlands[c]; Department of Cell Biology, The Netherlands Cancer Institute, Amsterdam, The Netherlands[d]

In response to genotoxic stress, DNA damage checkpoints maintain the integrity of the genome by delaying cell cycle progression to allow for DNA repair. Here we show that the degradation of the basic helix-loop-helix (bHLH) transcription factor DEC1, a critical regulator of cell fate and circadian rhythms, controls the DNA damage response. During unperturbed cell cycles, DEC1 is a highly unstable protein that is targeted for proteasome-dependent degradation by the SCF$^{\beta TrCP}$ ubiquitin ligase in cooperation with CK1. Upon DNA damage, DEC1 is rapidly induced in an ATM/ATR-dependent manner. DEC1 induction results from protein stabilization via a mechanism that requires the USP17 ubiquitin protease. USP17 binds and deubiquitylates DEC1, markedly extending its half-life. Subsequently, during checkpoint recovery, DEC1 proteolysis is reestablished through βTrCP-dependent ubiquitylation. Expression of a degradation-resistant DEC1 mutant prevents checkpoint recovery by inhibiting the downregulation of p53. These results indicate that the regulated degradation of DEC1 is a key factor controlling the DNA damage response.

Cells respond to genotoxic stress by activating DNA damage checkpoints, molecular networks that monitor the integrity of the genome before cells commit to either duplicating their DNA in S phase or separating their chromosomes in mitosis. Once DNA damage is sensed, cells temporarily stop cycling, facilitating DNA repair. If the degree of the DNA lesions exceeds the capacity of repair processes, cells die by apoptosis or exit irreversibly the cell division cycle and undergo senescence. The molecular mechanisms controlling the DNA damage response are of considerable interest not only because unrepaired DNA damage underlies the development of cancer and checkpoints represent critical barriers to tumor formation but also because DNA damage is employed therapeutically to kill cancer cells.

Many studies have shown that upon DNA damage, two major molecular cascades activated by the sensory ATM/ATR/DNA-protein kinase (PK) kinases are responsible for the arrest in the G_2 phase of the cell cycle (1–4). They converge to control the activity of the cyclin B/Cdk1 complex, the main regulator of the G_2/M transition. The first cascade, which rapidly prevents mitotic entry, involves the activation of the checkpoint kinases Chk1 and Chk2, which, in turn, phosphorylate and inactivate (or target for proteasome-dependent degradation) Cdc25 phosphatases, leading to the inhibition of Cdk1. The second, slower cascade involves the phosphorylation of p53, which impairs its interaction to the MDM2 ubiquitin ligase, promoting both the accumulation and activation of p53. Once induced, p53 target genes, such as the p21, 14-3-3, and GADD45 genes, contribute to blocking the activity of cyclin B/CDK1 through multiple mechanisms.

Basic helix-loop-helix (bHLH) transcription factors are key regulators of cell fate specification, apoptosis, cell proliferation, and metabolism (5–7). DEC1 (differentiated embryo-chondrocyte expressed gene 1 protein), also known as BHLHE40 (basic helix-loop-helix family, member e40), SHARP2 (enhancer of split and hairy related protein 2), and STRA13 (stimulated with retinoic acid 13), binds to E boxes and functions as a transcriptional repressor through histone deacetylase-dependent and -independent mechanisms (8, 9). It was originally identified as a retinoic acid-inducible protein that inhibits mesodermal differentiation and promotes neuronal differentiation (10). Subsequently, DEC1 was shown to have an important role in the regulation of mammalian circadian rhythms by repressing CLOCK/BMAL-dependent transactivation of gene expression (11–13). Interestingly, DEC1 expression is induced by a variety of clock-resetting stimuli such as light (in the suprachiasmatic nucleus), feeding (in the liver), serum shock, forskolin, transforming growth factor β (TGF-β), and phorbol 12-myristate 13-acetate (PMA) (in cultured cells), suggesting that DEC1 plays a key role in how the circadian clock senses the environment (13).

Besides confirming that DEC1 controls the circadian clock in mammals (12), *in vivo* studies have demonstrated that DEC1 is essential for T cell activation-induced cell death (AICD). Indeed, DEC1 deficiency in mice results in defective clearance of activated T and B cells, which accumulate progressively, causing lymphoid organ hyperplasia and systemic autoimmune disease (14).

Depending on the cellular context and the specific stimuli, DEC1 was also shown to mediate cell cycle arrest, senescence, and apoptosis via p53-dependent and -independent mechanisms (8, 14–16).

In this study, we showed that DEC1 degradation plays a critical

Received 18 April 2014 **Returned for modification** 7 May 2014
Accepted 11 August 2014
Published ahead of print 8 September 2014
Address correspondence to Daniele Guardavaccaro, d.guardavaccaro@hubrecht.eu.
Supplemental material for this article may be found at http://dx.doi.org/10.1128/MCB.00530-14.

doi:10.1128/MCB.00530-14

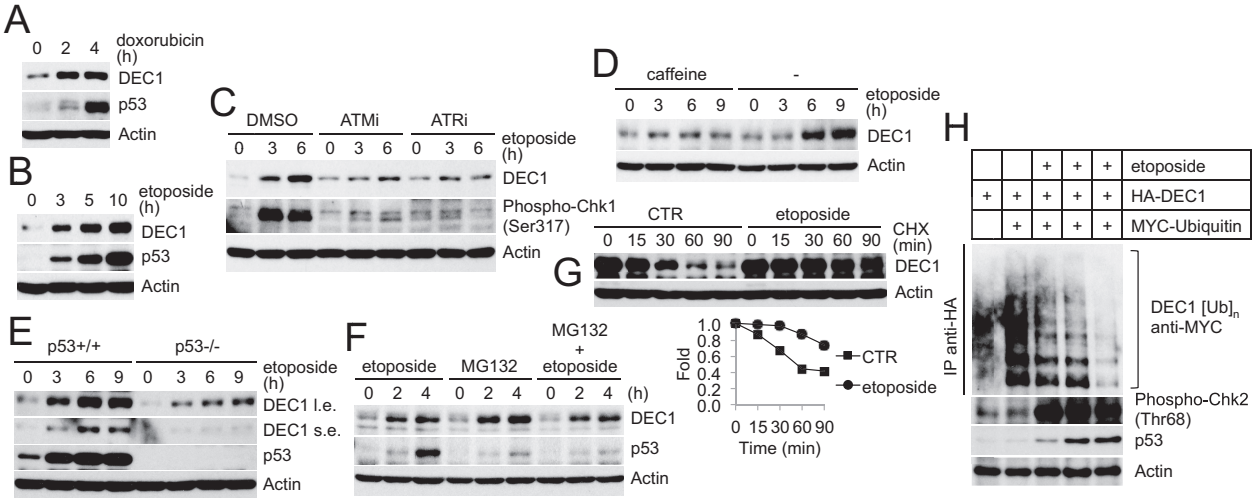

FIG 1 DEC1 protein levels are upregulated in response to genotoxic stress. (A and B) U2OS cells were treated with doxorubin (A) or etoposide (B) for the indicated times. Cells were collected and lysed. Whole-cell extracts were analyzed by immunoblotting with antibodies for the indicated proteins. Actin is shown as a loading control. (C) U2OS cells were treated with etoposide in the presence or absence of KU55933 (ATM inhibitor) or ATR-45 (ATR inhibitor) for the indicated times and then collected, lysed, and analyzed by immunoblotting. Dimethyl sulfoxide (DMSO) was used as a control. (D) HCT116 cells were treated with etoposide in the presence or absence of caffeine for the indicated times and then collected, lysed, and analyzed by immunoblotting. (E) HCT116 $p53^{+/+}$ and HCT116 $p53^{-/-}$ cells were treated with etoposide and collected at the indicated times. Cells were lysed and analyzed by immunoblotting (l.e., long exposure; s.e., short exposure). (F) U2OS cells were treated with the indicated compounds, alone or in combination, and collected at the indicated times. Whole-cell extracts were analyzed by immunoblotting with the indicated antibodies. (G) U2OS cells were pulse treated with etoposide. After the pulse, the inhibitor of protein synthesis cycloheximide (CHX) was added, and cells were collected at the indicated times. Whole-cell extracts were analyzed by immunoblotting with the indicated antibodies. DEC1 protein levels are quantified in the graph. CTR, DMSO-treated control. (H) U2OS cells expressing HA-tagged DEC1 and MYC-tagged ubiquitin were treated with etoposide. Whole-cell extracts were immunoprecipitated (IP) under denaturing conditions with an anti-HA resin. DEC1 immunoprecipitates were immunoblotted with an anti-MYC antibody to detect ubiquitylated DEC1. The bracket indicates a ladder of bands corresponding to polyubiquitylated DEC1. Phospho-Chk2 (Thr68) and p53 are shown as markers of checkpoint activation.

role in the DNA damage response. Genotoxic stress induces DEC1 stabilization via the USP17 ubiquitin protease. During recovery from the DNA damage checkpoint, DEC1 is targeted for proteasomal degradation by the $SCF^{\beta TrCP}$ ubiquitin ligase in cooperation with CK1α. Importantly, inhibition of DEC1 degradation slows down recovery from the G_2 DNA damage checkpoint by preventing p53 downregulation.

MATERIALS AND METHODS

Cell culture and drug treatment. U2OS, HEK293T, HEK293-GP2, HCT116, HCT116 $p53^{-/-}$, T98G, hTERT-RPE1, and hTERT-RPE1-FUCCI cells were maintained in Dulbecco's modified Eagle's medium (Invitrogen) containing 10% fetal calf serum, 100 U/ml of penicillin, and 100 U/ml streptomycin. The following drugs were used: etoposide (Sigma-Aldrich; 20 μg/ml), doxorubicin (Sigma-Aldrich; 0.125 μM for spontaneous recovery and 1 mM for caffeine-induced recovery), MG132 (Peptide Institute; 10 μM), tetrabromobenzotriazole (TBB; EMD Millipore, 75 μM), D4476 (Sigma-Aldrich; 50 μM), IC261 (Sigma-Aldrich; 50 μM), cycloheximide (Sigma-Aldrich; 100 μg/ml), caffeine (Sigma-Aldrich; 5 μM), thymidine (Sigma-Aldrich; 2.5 μM), nocodazole (Sigma-Aldrich; 0.1 μg/ml), KU55933 (ATM inhibitor; EMD Millipore; 10 μM), and ATR-45 (ATR inhibitor; Ohio State University; 2 μM).

Biochemical methods. Extract preparation, immunoprecipitation, and immunoblotting were done as previously described (17, 18). Mouse monoclonal antibodies were from Cell Signaling (phospho-p53 [Ser15]), Invitrogen (Cul1), Sigma-Aldrich (FLAG), BD Transduction Laboratories (p27), Santa Cruz Biotechnology (actin), and Covance (hemagglutinin [HA]). Rabbit polyclonal antibodies were from Cell Signaling (βTrCP1, CK1α, p53, MYC, phospho-Chk2 [Thr68]), Sigma-Aldrich (FLAG and USP8), Novus Biologicals (DEC1 and USP17), Santa Cruz Biotechnology (cyclin A), and EMD Millipore (phospho-histone H3 [Ser10]).

To generate the anti-DEC1 phosphospecific antibody (Ser243), rabbits were immunized with the SDTDTDpSGYGG phosphopeptide (where pS stands for phospho-Ser243). The rabbit polyclonal antiserum was purified through a two-step purification process. First, the antiserum was passed through a column containing the unphosphorylated peptide (SD TDTDSGYGG) to remove antibodies that recognize the unphosphorylated peptide. The flowthrough was then purified against the phosphopeptide to isolate antibodies that recognize DEC1 phosphorylated on Ser243. The final product was dialyzed with phosphate-buffered saline (PBS), concentrated, and tested for phosphopeptide and phosphoprotein specificity.

Purification of DEC1 interactors. HEK293T cells were transfected with pcDNA3-FLAG-HA-DEC1 and treated with 10 μM MG132 for 5 h. Cells were harvested and subsequently lysed in lysis buffer (50 mM Tris-HCl [pH 7.5], 150 mM NaCl, 1 mM EDTA, 0.5% NP-40, and protease and phosphatase inhibitors). DEC1 was immunopurified with anti-FLAG agarose resin (Sigma-Aldrich). After a washing, proteins were eluted by competition with FLAG peptide (Sigma-Aldrich). The eluate was then subject to a second immunopurification with anti-HA resin (12CA5 monoclonal antibody cross-linked to protein G-Sepharose; Invitrogen) prior to elution in Laemmli sample buffer. The final eluate was separated by SDS-PAGE, and proteins were visualized by Coomassie colloidal blue. Bands were sliced out from the gels and subjected to in-gel digestion. Gel pieces were then reduced, alkylated, and digested according to a published protocol (19). For mass spectrometric analysis, peptides recovered from in-gel digestion were separated with a C_{18} column and introduced by nanoelectrospray into the LTQ Orbitrap XL (Thermo Fisher) with a configuration described previously (20). Peak lists were generated from the tandem mass spectrometry (MS/MS) spectra using MaxQuant build 1.0.13.13 (21) and then searched against the IPI Human database (version 3.37; 69,164 entries) using the Mascot search engine (Matrix Science). Carbamidomethylation (+57 Da) was set as a fixed modification and

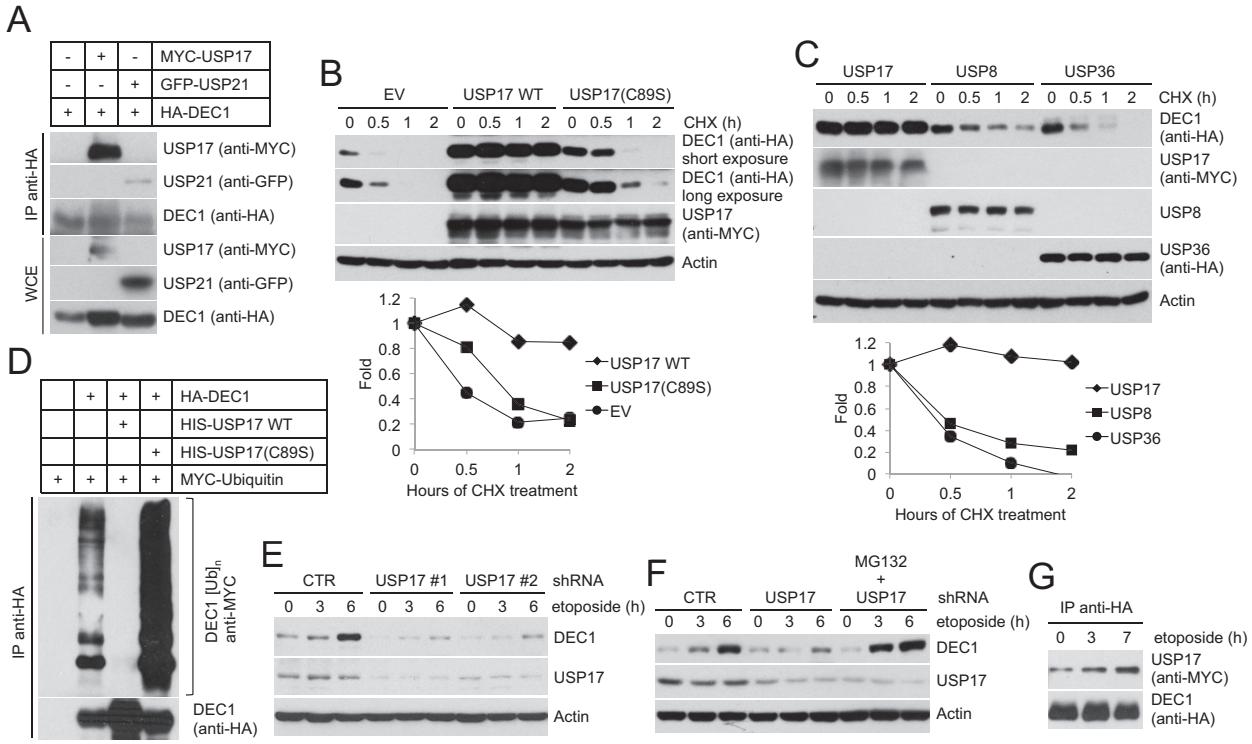

FIG 2 USP17 mediates the stabilization of DEC1 in response to DNA damage. (A) HEK293T cells were transfected with the indicated cDNAs. Cells were lysed and whole-cell extracts were subjected to immunoprecipitation using anti-HA resin before immunoblotting with antibodies for the indicated proteins. (B and C) Cells were transfected with the indicated constructs. After 48 h, cells were treated with cycloheximide (CHX) to block protein synthesis. Cells were collected at the indicated times and lysed. Whole-cell extracts were subjected to immunoblotting with antibodies specific for the indicated proteins. DEC1 abundance is quantified in the graphs. EV, empty vector. (D) HEK293T cells were transfected with the indicated constructs and culture in the presence of MG132 for 3 h. Cells were collected and lysed. Whole-cell extracts were prepared under denaturing conditions and subjected to immunoprecipitation with anti-HA resin. Immunocomplexes were then analyzed by immunoblotting with an anti-MYC antibody. The bracket indicates a ladder of bands corresponding to polyubiquitylated DEC1. (E and F) U2OS cells were transfected with constructs expressing either USP17 or control shRNAs. Cells were then treated with etoposide for the indicated times in the absence (E) or presence (F) of the proteasome inhibitor MG132 (where indicated). Cells were collected at the indicated times and lysed. Whole-cell extracts were analyzed by immunoblotting with antibodies specific for the indicated proteins. (G) U2OS cells expressing MYC-tagged USP17 and HA-tagged DEC1 were treated with etoposide for the indicated times. Cells were lysed and whole-cell extracts were immunoprecipitated with anti-HA resin. Immunoprecipitates were then analyzed by immunoblotting with antibodies specific for the indicated proteins.

protein N-terminal acetylation and methionine oxidation as variable modifications. To filter out false positives, all MS/MS spectra were searched against a forward and a reverse (decoy) protein database. All peptide-spectrum matches (PSMs) containing both forward and decoy hits were then trained and validated with an algorithm named Percolator (22), which uses semisupervised machine learning to discriminate between the correct and decoy matches. Finally, we accepted only PSMs based on a high stringency filter with a *q* value of 0.01 or a 1% false discovery rate (FDR). The 1% FDR filter is currently the standard for the proteomics community.

Plasmids and shRNAs. Mammalian expression plasmids for CK1α, His-USP17, MYC-USP17, USP8, and HA-USP36 were provided by H. Clevers, J. Johnston, K. Baek, M. Donzelli, and M. Komada, respectively. DEC1 cDNAs (wild type and mutants) were cloned in pcDNA3.1. For retrovirus production, HA-tagged DEC1 and MYC-tagged USP17 cDNAs (wild type and mutants) were subcloned into pBABE-PURO. DEC1 mutants were generated using the QuikChange site-directed mutagenesis kit (Stratagene). Small hairpin RNAs (shRNAs) targeting human CK1α were provided by W. Wei (23). The shRNAs for USP17, CCAAGACGTTAAC TTTACA (construct 1) and GCAGGAAGATGCCCATGAA (construct 2), were cloned in pSUPER. All constructs were sequenced.

Transient transfections and retrovirus- and lentivirus-mediated transfer. HEK293T and U2OS cells were transfected using the polyethylenimine (PEI) method. For retrovirus production, HEK293-GP2 cells were cotransfected with pBABE-puro-HA DEC1 and packaging vectors, and the virus-containing medium was collected after 48 h and supplemented with 8 μg/ml of Polybrene. For lentivirus production, HEK293T cells were transfected with pLKO-CK1 and packaging vectors. Virus-containing medium was collected 48 h after transfection and supplemented with 8 μg/ml of Polybrene. Target cells were incubated with the virus for 6 h.

Gene silencing by small interfering RNA (siRNA). The sequence and validation of oligonucleotides corresponding to βTrCP1 and βTrCP2 have been previously published (17, 24). Cells were transfected with the oligonucleotides twice (24 and 48 h after plating) using Oligofectamine (Invitrogen) according to the manufacturer's recommendations. Forty-eight hours after the last transfection, lysates were prepared and analyzed by SDS-PAGE and immunoblotting.

***In vitro* ubiquitylation assay.** DEC1 ubiquitylation was performed in a volume of 10 μl containing $SCF^{\beta TrCP}$-DEC1 immunocomplexes, 50 mM Tris (pH 7.6), 5 mM $MgCl_2$, 0.6 mM dithiothreitol (DTT), 2 mM ATP, 1.5 ng/μl of E1 (Boston Biochem), 10 ng/μl of Ubc3 (Boston Biochem), 2.5 μg/μl of ubiquitin (Sigma-Aldrich), and 1 μM ubiquitin aldehyde. The reaction mixtures were incubated at 30°C for 60 min and analyzed by immunoblotting.

Live-cell microscopy. Time-lapse microscopy to analyze mitotic entry was performed as described previously (25, 26).

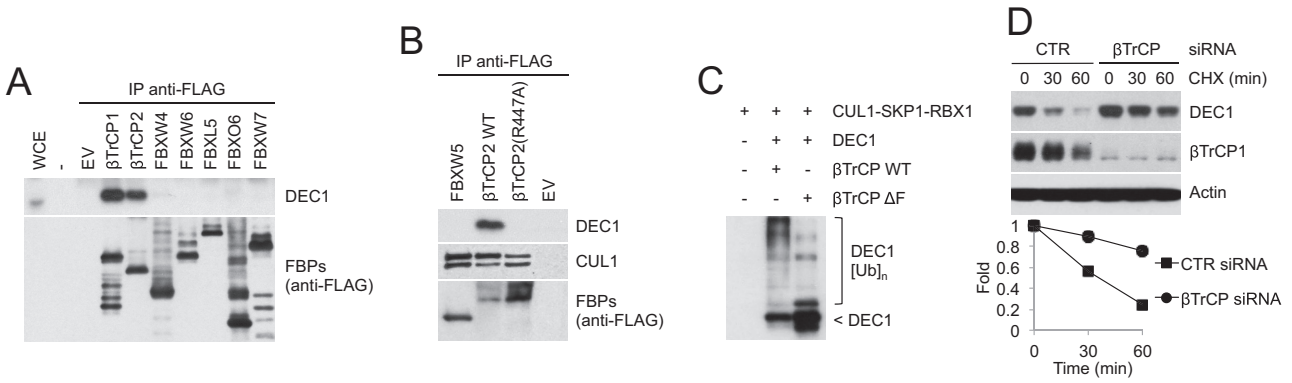

FIG 3 DEC1 degradation is controlled by the $SCF^{\beta TrCP}$ ubiquitin ligase. (A) βTrCP1 and βTrCP2 interact with DEC1. The indicated FLAG-tagged F box proteins (FBPs) or an empty vector (EV) were expressed in HEK293T cells. Forty-eight hours after transfection, cells were treated for 5 h with the proteasome inhibitor MG132 and then harvested and lysed. Whole-cell extracts were immunoprecipitated with anti-FLAG resin and immunoblotted with the indicated antibodies. (B) Arg447 in the WD40 repeat of βTrCP2 is required for βTrCP2 binding to DEC1. HEK293T cells were transfected as indicated. After 48 h, cells were treated with MG132 for 5 h and then harvested and lysed. Whole-cell extracts (WCE) were subjected to immunoprecipitation with anti-FLAG resin, followed by immunoblotting with antibodies specific for the indicated proteins (WT, wild type). (C) DEC1 is ubiquitylated by $SCF^{\beta TrCP}$ *in vitro*. DEC1, Skp1, Cul1, and Rbx1 were expressed in HEK293T cells in the absence or presence of either FLAG-tagged βTrCP1 or a FLAG-tagged βTrCP1(ΔF box) mutant. After immunopurification with anti-FLAG resin, *in vitro* ubiquitylation of DEC1 was performed. Samples were analyzed by immunoblotting with an anti-DEC1 antibody. The bracket indicates a ladder of bands corresponding to polyubiquitylated DEC1. (D) Cells were transfected with the indicated siRNA oligonucleotides and treated with cycloheximide. Cells were then collected at the indicated times and lysed. Whole-cell extracts were subjected to immunoblotting with antibodies specific for the indicated proteins. Actin is shown as a loading control. DEC1 expression is quantified in the graph.

Statistical analysis. All data shown are from one representative experiment of at least three performed. Statistical analysis was performed using Student's *t* test. Results with *P* values of <0.005 were considered to be statistically significant.

RESULTS

DEC1 is induced by DNA damage in an ATM/ATR-dependent manner. It has been shown that genotoxic stress triggers the induction of DEC1 (15, 16, 27). We first confirmed these results by showing that DEC1 is rapidly induced by doxorubicin and etoposide, two topoisomerase inhibitors that cause DNA double-strand breaks (Fig. 1A and B). To extend our observations, we examined the effect of pharmacological inhibition of ATM and ATR, main effector kinases of the DNA damage response, on the induction of DEC1 in response to genotoxic stress. Inhibition of either ATM or ATR prevented the increase of DEC1 protein levels upon etoposide treatment (Fig. 1C). Similarly, treatment of cells with caffeine, which blocks the activation of the ATM and ATR kinases, inhibited the induction of DEC1 upon genotoxic stress (Fig. 1D). To test whether the increase in DEC1 following a DNA damage insult depends on p53, we compared the levels of DEC1 in etoposide-treated HCT116 $p53^{+/+}$ cells with the ones in HCT116 $p53^{-/-}$ cells (Fig. 1E). Although the levels of DEC1 are overall lower in the absence of p53, DEC1 was induced with similar kinetics in HCT116 $p53^{-/-}$ and HCT116 $p53^{+/+}$ cells (compare long and short exposure times of DEC1 immunoblotting).

A number of factors suggest that the induction of DEC1 in response to genotoxic stress is due to regulation of its turnover. First, proteasome inhibition and DNA damage in U2OS cells cause similar increases in DEC1 levels (Fig. 1F). Second, MG132 treatment of damaged cells does not cause a further increase of DEC1 levels (Fig. 1F). Third, and more importantly, the half-life of DEC1 is extended by etoposide treatment (Fig. 1G).

DEC1 stabilization in response to genotoxic stress might be due to regulation of its ubiquitylation. To test this possibility, we analyzed the ubiquitylation of DEC1 in U2OS cells treated with etoposide. As shown in Fig. 1H, the activation of the DNA damage response by etoposide treatment (monitored by the induction of p53 and phospho-Chk2 [Thr68]) was associated with a decrease in DEC1 ubiquitylation.

USP17 is required for the stabilization of DEC1 in response to genotoxic stress. To identify DEC1-interacting proteins that may play a role in the regulation of DEC1 ubiquitylation and degradation, FLAG-HA-tagged DEC1 was expressed in HEK293T cells, immunopurified, and analyzed by mass spectrometry. We recovered peptides corresponding to the USP17 deubiquitylating enzyme as well as the subunits of the $SCF^{\beta TrCP}$ ubiquitin ligase, i.e., Skp1, Cul1, Rbx1, βTrCP1, and βTrCP2 (see Table S1 in the supplemental material).

We first confirmed the binding between USP17 and DEC1 (Fig. 2A). Next, to test whether USP17 controls the stability of DEC1, we expressed DEC1 along with USP17 in U2OS cells and blocked protein synthesis by cycloheximide treatment. As shown in Fig. 2B, expression of USP17 but not of a USP17 mutant in which the catalytic cysteine has been replaced by serine (C89S) markedly stabilized DEC1. Expression of other deubiquitylating enzymes such as USP8 or USP36 had no effect on DEC1 turnover (Fig. 2C). Moreover, wild-type USP17, but not the catalytically inactive USP17 (C89S) mutant, reduced the amount of ubiquitylated DEC1 in cultured cells (Fig. 2D).

These results suggest that USP17 might be responsible for the stabilization of DEC1 observed in response to genotoxic stress. To test this hypothesis, we depleted USP17 using RNA interference (RNAi) and examined the levels of DEC1 following DNA damage. The knockdown of USP17 in etoposide-treated cells inhibited the induction of DEC1 (Fig. 2E), which was rescued by proteasome inhibition (Fig. 2F). Next, we tested whether the physical interaction between DEC1 and USP17 is regulated by genotoxic stress. Figure 2G shows that treatment of U2OS cells with etoposide stimulates the association of USP17 with DEC1.

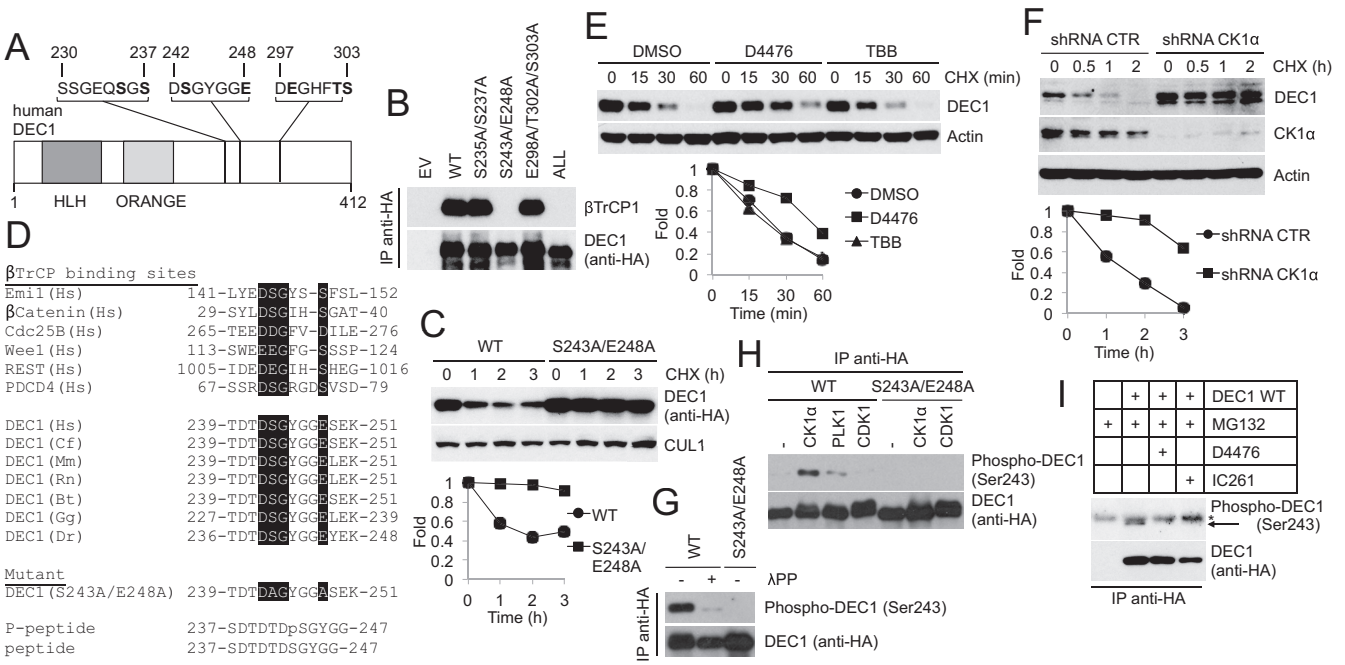

FIG 4 CK1α-mediated phosphorylation of DEC1 on a conserved degron is required for DEC1 degradation. (A) DEC1 contains three potential βTrCP-binding domains. The amino acid residues that were mutated to alanine are shown in bold. (B) HEK293T cells were transfected with an empty vector, HA-tagged wild-type DEC1, or the indicated HA-tagged DEC1 mutants. Forty-eight hours after transfection, cells were harvested and lysed. Whole-cell extracts were subjected to immunoprecipitation with anti-HA resin, followed by immunoblotting with antibodies specific for the indicated proteins. (C) HEK293T cells were transfected with the indicated constructs. After 24 h, cells were treated with the inhibitor of protein synthesis cycloheximide and collected at the indicated times. Whole-cell extracts were then immunoblotted with the indicated antibodies. DEC1 expression is quantified in the graph below. (D) (Top) alignment of the amino acid regions corresponding to the βTrCP-binding motif (highlighted in black) in previously reported βTrCP substrates and DEC1 orthologs. The amino acid sequence of the DEC1 double mutant is shown. (Bottom) Sequence of the phosphopeptide and the corresponding unphosphorylated peptide used to generate the anti-DEC1 phosphospecific antibody (Ser243). Hs, *Homo sapiens*; Cf, *Canis familiaris*; Mm, *Mus musculus*; Rn, *Rattus norvegicus*; Bt, *Bos taurus*; Gg, *Gallus gallus*; Dr, *Danio rerio*. (E) U2OS cells were treated with the indicated kinase inhibitors. Cells were collected at the indicated times and lysed. Whole-cell extracts were then immunoblotted with antibodies specific for the indicated proteins. Actin is shown as a loading control. DEC1 expression is quantified in the graph. (F) U2OS cells were transduced with the indicated lentiviral shRNA vectors. Cells were then treated with cycloheximide for the indicated times. Cells were collected and lysed. Whole-cell extracts were analyzed by immunoblotting. DEC1 expression is quantified in the graph. (G) Immunoprecipitated wild-type DEC1 and DEC1(S243A/E248A) were analyzed by immunoblotting with antibodies specific for the indicated proteins. Where indicated, immunocomplexes were treated with lambda phosphatase (λPP) for 30 min. (H) Immunoprecipitated wild-type DEC1 and DEC1(S243A/E248A) were dephosphorylated by treatment with lambda phosphatase and then incubated with the indicated purified kinases in the presence of ATP. Reactions were stopped by adding Laemmli buffer and analyzed by immunoblotting with antibodies specific for the indicated proteins. (I) U2OS cells were transfected with HA-tagged wild-type DEC1. Forty-eight hours after transfection, cells were treated with either D4476 or IC261 (CK1 pharmacological inhibitors). Cells were then harvested and lysed. Whole-cell extracts were immunoprecipitated with anti-HA resin and analyzed by immunoblotting. The asterisk indicates a nonspecific band.

DEC1 is targeted for proteasome-dependent degradation by SCF$^{\beta TrCP}$. The identification of the SCF$^{\beta TrCP}$ subunits in the immunopurification of DEC1 (see Table S1 in the supplemental material) prompted us to assess the involvement of SCF$^{\beta TrCP}$ in the regulation of DEC1 proteolysis. To confirm the interaction of DEC1 with βTrCP, we immunoprecipitated a panel of F box proteins and tested their binding to endogenous DEC1. As shown in Fig. 3A, only βTrCP1 and βTrCP2 were able to coimmunoprecipitate endogenous DEC1. Furthermore, mutation of Arg447, a residue within the WD40 repeats of βTrCP2 required for interactions with its substrates (28, 29), prevented the binding of DEC1 to βTrCP (Fig. 3B). To test whether DEC1 is a substrate of SCF$^{\beta TrCP}$, we reconstituted the ubiquitylation of DEC1 *in vitro*. βTrCP1, but not an inactive βTrCP1(ΔF box) mutant, was able to mediate DEC1 ubiquitylation *in vitro* (Fig. 3C). To examine whether DEC1 stability is regulated by βTrCP, we reduced the expression of both βTrCP1 and βTrCP2 using a previously validated siRNA (28). As shown in Fig. 3D, the knockdown of βTrCP caused DEC1 stabilization in HEK293T cells. Together, these results indicate that DEC1 degradation is controlled by the SCF$^{\beta TrCP}$ ubiquitin ligase.

CK1α-mediated phosphorylation of DEC1 is required for its destruction. The binding of βTrCP to its substrates requires the phosphorylation of serine residues within a degron sequence. Some substrates of βTrCP have one or both serine residues replaced by either aspartic or glutamic acid (17, 30). DEC1 contains three putative βTrCP-binding domains (Fig. 4A). To assess which of these three domains mediates the binding of DEC1 to βTrCP, we generated a number of DEC1 double mutants with changes of serine, aspartic acid, or glutamic acid to alanine (all HA tagged) and examined their ability to interact with endogenous βTrCP. As shown in Fig. 4B, mutation of Ser243 and Glu248 to alanine prevented the binding of DEC1 to βTrCP, whereas mutation of the other two motifs had no effect on the DEC1-βTrCP interaction. Accordingly, the DEC1(S243A/E248A) mutant is stable in cultured HEK293T cells (Fig. 4C). The βTrCP-binding domain in DEC1 is conserved in different species (Fig. 4D).

DEC1 Ser243 is part of a conserved phosphorylation consensus

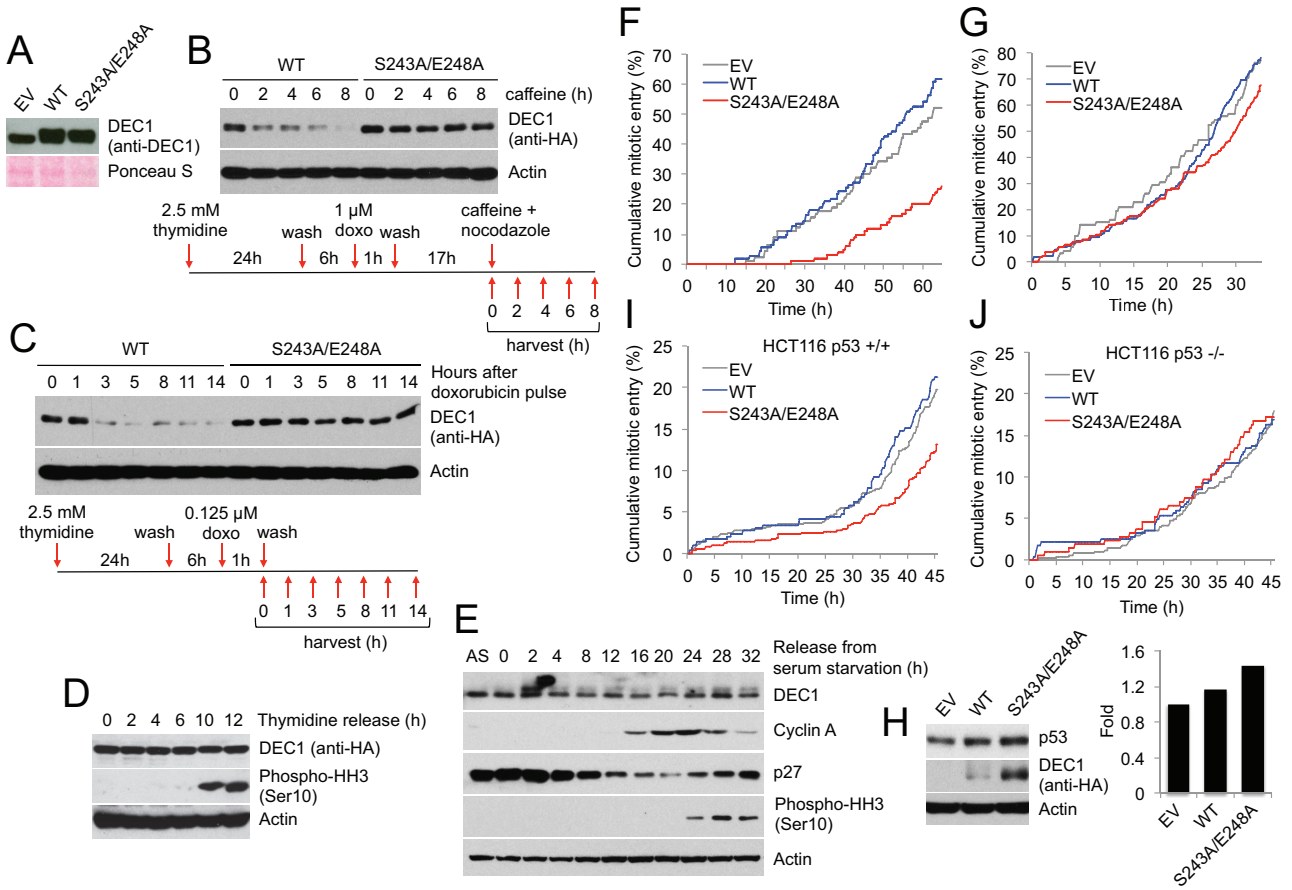

FIG 5 DEC1 degradation is required for checkpoint recovery. (A) U2OS cells were transduced with retroviruses expressing HA-tagged wild-type DEC1 or HA-tagged DEC1(S243A/E248A) or with an empty vector. Cells were then collected and analyzed by immunoblotting with an anti-DEC1 antibody. Staining of the polyvinylidene difluoride (PVDF) membrane with Ponceau S shows equal loading. (B) U2OS cells, transduced with retroviruses expressing HA-tagged wild-type DEC1 or HA-tagged DEC1(S243A/E248A), were treated according to the scheme shown. Cells were then collected and analyzed by immunoblotting with antibodies for the indicated proteins. Actin is shown as a loading control. (C) U2OS cells were treated as for panel B, except that doxorubicin was used at a lower dose (0.125 μM) and cells were left recovering spontaneously (without adding caffeine). Cells were then collected and analyzed by immunoblotting with antibodies for the indicated proteins. Actin is shown as a loading control. (D) U2OS cells expressing HA-tagged wild-type DEC1 were first synchronized at the G_1/S transition by thymidine block and then washed extensively and incubated in fresh medium (indicated as time zero) to allow progression through S, G_2, and mitosis. (E) T98G cells (revertants from T98 glioblastoma cells that acquired the property of accumulating in G_0/G1 in low serum) were synchronized in G_0 by serum deprivation (0) and released from the arrest by the addition of serum. AS, asynchronously growing cells. Cells were collected at the indicated time points and lysed. Whole-cell extracts were analyzed by immunoblotting with antibodies specific for the indicated proteins. (F) hTERT-RPE1 cells expressing HA-tagged wild-type DEC1, HA-tagged DEC1(S243A/E248A), or an empty vector were pulse treated (1 h) with 0.5 μM doxorubicin. Cells were monitored by time-lapse microscopy and scored for mitotic entry. (G) Asynchronously growing hTERT-RPE1 cells expressing wild-type DEC1, DEC1(S243A/E248A), or an empty vector were monitored by time-lapse microscopy and scored for mitotic entry. (H) Same as for panel F. Twenty-four hours after the pulse, cells were collected and analyzed by immunoblotting with antibodies specific for the indicated proteins. The expression of p53 is quantified in the graph. (I and J) HCT116 $p53^{+/+}$ (I) and HCT116 $p53^{-/-}$ (J) cells, expressing HA-tagged wild-type DEC1, HA-tagged DEC1(S243A/E248A), or an empty vector, were pulse treated (1 h) with 0.5 μM doxorubicin. Cells were then monitored by time-lapse microscopy and scored for mitotic entry.

site for casein kinase 1 (CK1). To test whether CK1 is involved in the degradation of DEC1, we treated cells with CK1 pharmacological inhibitors and analyzed the half-life of DEC1. Treatment of U2OS cells with D4476 (a CK1 inhibitor) but not TBB (a CK2 inhibitor) caused DEC1 stabilization (Fig. 4E). Furthermore, knockdown of CK1α by RNAi prevented DEC1 degradation in U2OS cells (Fig. 4F).

Next, we generated a phospho-specific antibody that recognizes DEC1 only when it is phosphorylated on Ser243 (Fig. 4D and G). We employed this antibody to test whether CK1α phosphorylates DEC1 on Ser243. DEC1 was immunopurified from HEK293T cells, dephosphorylated, and then subjected to phosphorylation *in vitro* in the presence of different purified kinases. As a control, we used the DEC1(S243A/E248A) mutant. DEC1 phosphorylation on Ser243 was then assessed by immunoblotting using the phosphospecific antibody that recognizes DEC1 only when it is phosphorylated on Ser243. Figure 4H shows that DEC1 Ser243 is specifically phosphorylated by CK1α. Accordingly, pharmacological inhibition of CK1 blocked Ser243 phosphorylation in cultured cells (Fig. 4I).

$SCF^{\beta TrCP}$ and CK1α trigger the degradation of DEC1 during checkpoint recovery. Our data demonstrate that $SCF^{\beta TrCP}$ and CK1α control the degradation of DEC1 and suggest that they may be involved not only in the constitutive turnover of DEC1 but also in its destruction during checkpoint recovery to counteract the USP17-mediated and DNA damage-induced stabilization of

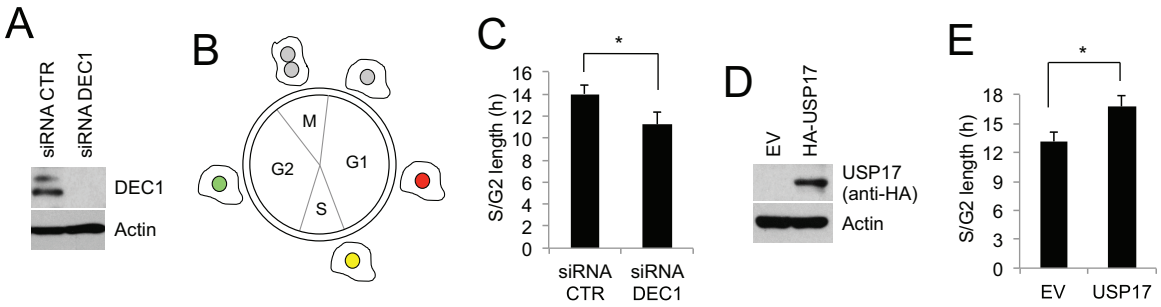

FIG 6 Role of USP17-mediated induction of DEC1 in the G_2 DNA damage checkpoint. (A) hTERT-RPE1-FUCCI cells were transfected with the indicated siRNAs. Whole-cell extracts were analyzed by immunoblotting with antibodies specific for the indicated proteins. (B and C) Cells as for panel A were pulsed treated (1 h) with doxorubicin and imaged by time-lapse microscopy. The duration of S/G_2 (GFP-positive cells) was measured. The graph indicates the quantification of the S/G_2 duration. Average values (±SD) are indicated. (D) hTERT-RPE1-FUCCI cells were transfected with HA-tagged USP17 or an empty vector. Whole-cell extracts were analyzed by immunoblotting with antibodies specific for the indicated proteins. (E) Cells as for panel D were pulsed treated (1 h) with doxorubicin and imaged by time-lapse microscopy. The duration of S/G_2 (GFP-positive cells) was measured. The graph indicates the quantification of the S/G_2 duration. Average values (±SD) are indicated.

DEC1. To test this possibility, we expressed physiological levels of wild-type DEC1 and the DEC1(S243A/E248A) mutant, which is unable to bind βTrCP in U2OS cells (Fig. 5A). Cells were then synchronized in G_2 and pulsed with doxorubicin to activate the G_2 DNA damage checkpoint. To induce checkpoint recovery, cells were then treated with caffeine, which inhibits the checkpoint kinases ATM and ATR, turning off the checkpoint. As shown in Fig. 5B, whereas wild-type DEC1 was rapidly degraded during caffeine-induced checkpoint recovery, the DEC1(S243A/E248A) mutant was stable. Similar results were obtained when cells were allowed to recover spontaneously from the G_2 DNA damage checkpoint that was activated by a lower dose of doxorubicin (Fig. 5C). In contrast, the abundance of wild-type DEC1 did not change when cells were released from the G_1/S border without DNA damage (Fig. 5D). In addition, no significant changes in the levels of endogenous DEC1 were observed in cells synchronized in G_0 by serum deprivation and released in serum-containing medium to allow synchronized progression through G_1, S, G_2, and mitosis (Fig. 5E).

Regulated degradation of DEC1 controls the G_2 DNA damage checkpoint. To study the biological effect of CK1α- and βTrCP-mediated degradation of DEC1 on checkpoint recovery, we analyzed the mitotic entry of hTERT-immortalized retinal pigment epithelial (RPE1) cells expressing either wild-type DEC1 or the degradation-resistant DEC1(S243A/E248A) mutant after a pulse of doxorubicin. As shown in Fig. 5F, hTERT-RPE1 cells expressing DEC1(S243A/E248A) displayed defective checkpoint recovery compared with control cells. Indeed, 60 h after the doxorubicin pulse, approximately 50% of control cells had entered mitosis, whereas only 20% of cells expressing the degradation-resistant DEC1 mutant had reached mitosis at that time. Failure to degrade DEC1 during unperturbed cell cycles had a minimal effect on mitotic entry (Fig. 5G).

It has been shown that DEC1 regulates the expression of p53 by directly interacting with p53, blocking its MDM2-mediated degradation (16). To test whether the defective recovery of cells expressing the nondegradable DEC1 mutant was associated with sustained levels of p53, we assessed the levels of p53 in cells expressing the degradation-resistant DEC1 mutant during checkpoint recovery. As shown in Fig. 5H, 24 h after the DNA damage pulse, cells expressing DEC1(S243A/E248A) displayed increased levels of p53 compared with those of cells expressing wild-type DEC1.

To demonstrate that the defective checkpoint recovery in cells expressing the degradation-resistant DEC1 mutant was indeed caused by the inability of these cells to downregulate p53, we analyzed the effect of defective DEC1 degradation on checkpoint recovery in p53-deficient HCT116 cells. Figure 5I and J show that the recovery from the G_2 DNA damage checkpoint is impaired by the expression of DEC1(S243A/E248A) in HCT116 $p53^{+/+}$ cells but not in HCT116 $p53^{-/-}$ cells.

Finally, we examined the role of the induction of DEC1 upon DNA damage. To this end, we silenced the expression of DEC1 by RNAi in hTERT-RPE1-FUCCI cells, which were then treated with a pulse of doxorubicin. These cells, which express both a red (RFP) and a green (GFP) fluorescent protein fused to the cell cycle regulators Cdt1 and geminin, respectively, allowed us to monitor the progression through cell cycle phases in response to genotoxic stress (31). Figure 6A to C indicate that the knockdown of DEC1 caused a defective G_2 DNA damage checkpoint, as doxorubicin-treated cells in which DEC1 was silenced have a shorter G_2 phase than do doxorubicin-treated control cells. In contrast, ectopic expression of USP17, which mediates the stabilization of DEC1 in response to DNA damage, leads to a prolonged G_2 checkpoint following treatment with doxorubicin (Fig. 6D and E).

DISCUSSION

In the present work, we show that the rapid induction of DEC1 in response to genotoxic stress is dependent on the USP17 deubiquitylating enzyme and that the proteasomal degradation of DEC1, mediated by $SCF^{\beta TrCP}$ and CK1α, is required for efficient recovery from the G_2 DNA damage checkpoint. In line with our findings, a recently performed large-scale comparative phosphoproteomic screen, aimed at analyzing changes in protein phosphorylation during checkpoint recovery and identifying factors required for this process, identified CK1α as a potential regulator of checkpoint recovery (32). Indeed, CK1α was found to be differentially phosphorylated during recovery from the G_2 checkpoint caused by DNA damage, and importantly, cells in which CK1α was depleted by siRNA were unable to recover from the DNA damage-induced G_2 arrest (32).

A number of studies have uncovered a key function of

$SCF^{\beta TrCP}$ in driving cells into mitosis during recovery from DNA replication and the DNA damage checkpoints. Indeed, during checkpoint recovery, $SCF^{\beta TrCP}$, in cooperation with Polo-like kinase-1, contributes to turning Cdk1 activity on by targeting both claspin and Wee1 for proteasomal degradation. Claspin is an adaptor protein that in response to DNA replication and DNA damage checkpoints promotes ATR-mediated phosphorylation and activation of Chk1. Claspin degradation triggered by βTrCP and Polo-like kinase-1 leads to Chk1 inactivation and subsequent accumulation of Cdc25A and activation of Cdc25B and Cdc25C. Wee1 is a direct inhibitor of Cdk1, and its destruction by βTrCP and Polo-like kinase-1 removes the break on Cdk1 activity. These degradation events, despite being crucial, are insufficient to account for the whole checkpoint recovery process. In fact, inactivation of p53, a second important brake responsible for a sustained cell cycle arrest upon genotoxic stress, is essential for checkpoint recovery. Our study indicates that by targeting DEC1 for degradation during recovery from the G_2 checkpoint, $SCF^{\beta TrCP}$ is also responsible for the termination of the inhibitory action of p53 on G_2 progression and mitotic entry.

Interestingly, a genome-wide characterization of DEC1-regulated genes in T lymphocytes has been recently reported (33). Gene ontology analysis revealed that cell cycle genes, in particular genes that control the G_2/M transition, were highly enriched (third highest category) among the DEC1-regulated genes, implying that in addition to its effect on p53 expression, DEC1-regulated stability in response to DNA damage might modulate the expression of a multitude of genes controlling cell cycle progression.

Finally, as DEC1 is a crucial regulator of circadian rhythms, our findings suggest that acute induction of DEC1 in response to genotoxic stress, carried out by the coordinated actions of USP17 and $CK1\alpha/SCF^{\beta TrCP}$, might enable a rapid resetting of the circadian clock following DNA damage.

ACKNOWLEDGMENTS

We thank K. Baek and J. Johnston for reagents and the Hubrecht Imaging Center (HIC) for contribution.

Work in D.G.'s laboratory was supported by the Royal Dutch Academy of Arts and Sciences (KNAW), the Dutch Cancer Society (KWF), the Cancer Genomics Centre, and the European Union under Marie Curie Actions (FP7). T.Y.L., S.M., and A.J.R.H. were supported by the Netherlands Proteomics Center (NPC).

We declare that we have no competing financial interests and no other conflicts of interest.

J.K. contributed to the design, execution, and analysis of most experiments and helped write the manuscript. D.G. contributed to the concept, design, and analysis of the experiments, provided funding, and wrote the manuscript. All other authors contributed to the execution and/or analysis of specific experiments.

REFERENCES

1. **Medema RH, Macurek L.** 2012. Checkpoint control and cancer. Oncogene **31:**2601–2613. http://dx.doi.org/10.1038/onc.2011.451.
2. **Jackson SP, Bartek J.** 2009. The DNA-damage response in human biology and disease. Nature **461:**1071–1078. http://dx.doi.org/10.1038/nature08467.
3. **Kastan MB, Bartek J.** 2004. Cell-cycle checkpoints and cancer. Nature **432:**316–323. http://dx.doi.org/10.1038/nature03097.
4. **Harper JW, Elledge SJ.** 2007. The DNA damage response: ten years after. Mol. Cell **28:**739–745. http://dx.doi.org/10.1016/j.molcel.2007.11.015.
5. **Murre C, McCaw PS, Vaessin H, Caudy M, Jan LY, Jan YN, Cabrera CV, Buskin JN, Hauschka SD, Lassar AB, Weintraub H, Baltimore D.** 1989. Interactions between heterologous helix-loop-helix proteins generate complexes that bind specifically to a common DNA sequence. Cell **58:**537–544. http://dx.doi.org/10.1016/0092-8674(89)90434-0.
6. **Atchley WR, Fitch WM.** 1997. A natural classification of the basic helix-loop-helix class of transcription factors. Proc. Natl. Acad. Sci. U. S. A. **94:**5172–5176. http://dx.doi.org/10.1073/pnas.94.10.5172.
7. **Ledent V, Paquet O, Vervoort M.** 2002. Phylogenetic analysis of the human basic helix-loop-helix proteins. Genome Biol. **3:**RESEARCH0030. http://dx.doi.org/10.1186/gb-2002-3-6-research0030.
8. **Sun H, Taneja R.** 2000. Stra13 expression is associated with growth arrest and represses transcription through histone deacetylase (HDAC)-dependent and HDAC-independent mechanisms. Proc. Natl. Acad. Sci. U. S. A. **97:**4058–4063. http://dx.doi.org/10.1073/pnas.070526297.
9. **St-Pierre B, Flock G, Zacksenhaus E, Egan SE.** 2002. Stra13 homodimers repress transcription through class B E-box elements. J. Biol. Chem. **277:**46544–46551. http://dx.doi.org/10.1074/jbc.M111652200.
10. **Boudjelal M, Taneja R, Matsubara S, Bouillet P, Dolle P, Chambon P.** 1997. Overexpression of Stra13, a novel retinoic acid-inducible gene of the basic helix-loop-helix family, inhibits mesodermal and promotes neuronal differentiation of P19 cells. Genes Dev. **11:**2052–2065. http://dx.doi.org/10.1101/gad.11.16.2052.
11. **Honma S, Kawamoto T, Takagi Y, Fujimoto K, Sato F, Noshiro M, Kato Y, Honma K.** 2002. Dec1 and Dec2 are regulators of the mammalian molecular clock. Nature **419:**841–844. http://dx.doi.org/10.1038/nature01123.
12. **Nakashima A, Kawamoto T, Honda KK, Ueshima T, Noshiro M, Iwata T, Fujimoto K, Kubo H, Honma S, Yorioka N, Kohno N, Kato Y.** 2008. DEC1 modulates the circadian phase of clock gene expression. Mol. Cell. Biol. **28:**4080–4092. http://dx.doi.org/10.1128/MCB.02168-07.
13. **Kon N, Hirota T, Kawamoto T, Kato Y, Tsubota T, Fukada Y.** 2008. Activation of TGF-beta/activin signalling resets the circadian clock through rapid induction of Dec1 transcripts. Nat. Cell Biol. **10:**1463–1469. http://dx.doi.org/10.1038/ncb1806.
14. **Sun H, Lu B, Li RQ, Flavell RA, Taneja R.** 2001. Defective T cell activation and autoimmune disorder in Stra13-deficient mice. Nat. Immunol. **2:**1040–1047. http://dx.doi.org/10.1038/ni721.
15. **Qian Y, Zhang J, Yan B, Chen X.** 2008. DEC1, a basic helix-loop-helix transcription factor and a novel target gene of the p53 family, mediates p53-dependent premature senescence. J. Biol. Chem. **283:**2896–2905. http://dx.doi.org/10.1074/jbc.M708624200.
16. **Thin TH, Li L, Chung TK, Sun H, Taneja R.** 2007. Stra13 is induced by genotoxic stress and regulates ionizing-radiation-induced apoptosis. EMBO Rep. **8:**401–407. http://dx.doi.org/10.1038/sj.embor.7400912.
17. **Guardavaccaro D, Frescas D, Dorrello NV, Peschiaroli A, Multani AS, Cardozo T, Lasorella A, Iavarone A, Chang S, Hernando E, Pagano M.** 2008. Control of chromosome stability by the beta-TrCP-REST-Mad2 axis. Nature **452:**365–369. http://dx.doi.org/10.1038/nature06641.
18. **Ping Z, Lim R, Bashir T, Pagano M, Guardavaccaro D.** 2012. APC/C (Cdh1) controls the proteasome-mediated degradation of E2F3 during cell cycle exit. Cell Cycle **11:**1999–2005. http://dx.doi.org/10.4161/cc.20402.
19. **Shevchenko A, Wilm M, Vorm O, Mann M.** 1996. Mass spectrometric sequencing of proteins silver-stained polyacrylamide gels. Anal. Chem. **68:**850–858. http://dx.doi.org/10.1021/ac950914h.
20. **Raijmakers R, Berkers CR, de Jong A, Ovaa H, Heck AJ, Mohammed S.** 2008. Automated online sequential isotope labeling for protein quantitation applied to proteasome tissue-specific diversity. Mol. Cell. Proteomics **7:**1755–1762. http://dx.doi.org/10.1074/mcp.M800093-MCP200.
21. **Cox J, Mann M.** 2008. MaxQuant enables high peptide identification rates, individualized p.p.b.-range mass accuracies and proteome-wide protein quantification. Nat. Biotechnol. **26:**1367–1372. http://dx.doi.org/10.1038/nbt.1511.
22. **Käll L, Canterbury JD, Weston J, Noble WS, MacCoss MJ.** 2007. Semi-supervised learning for peptide identification from shotgun proteomics datasets. Nat. Methods **4:**923–925. http://dx.doi.org/10.1038/nmeth1113.
23. **Gao D, Inuzuka H, Tan MK, Fukushima H, Locasale JW, Liu P, Wan L, Zhai B, Chin YR, Shaik S, Lyssiotis CA, Gygi SP, Toker A, Cantley LC, Asara JM, Harper JW, Wei W.** 2011. mTOR drives its own activation via SCF(betaTrCP)-dependent degradation of the mTOR inhibitor DEPTOR. Mol. Cell **44:**290–303. http://dx.doi.org/10.1016/j.molcel.2011.08.030.
24. **D'Annibale S, Kim J, Magliozzi R, Low TY, Mohammed S, Heck AJ, Guardavaccaro D.** 2014. Proteasome-dependent degradation of tran-

scription factor AP4 (TFAP4) controls mitotic division. J. Biol. Chem. **289:**7730–7737. http://dx.doi.org/10.1074/jbc.M114.549535.

25. **Lindqvist A, de Bruijn M, Macurek L, Bras A, Mensinga A, Bruinsma W, Voets O, Kranenburg O, Medema RH.** 2009. Wip1 confers G2 checkpoint recovery competence by counteracting p53-dependent transcriptional repression. EMBO J. **28:**3196–3206. http://dx.doi.org/10.1038/emboj.2009.246.
26. **Alvarez-Fernández M, Halim VA, Krenning L, Aprelia M, Mohammed S, Heck AJ, Medema RH.** 2010. Recovery from a DNA-damage-induced G2 arrest requires Cdk-dependent activation of FoxM1. EMBO Rep. **11:**452–458. http://dx.doi.org/10.1038/embor.2010.46.
27. **Qian Y, Jung YS, Chen X.** 2012. Differentiated embryo-chondrocyte expressed gene 1 regulates p53-dependent cell survival versus cell death through macrophage inhibitory cytokine-1. Proc. Natl. Acad. Sci. U. S. A. **109:**11300–11305. http://dx.doi.org/10.1073/pnas.1203185109.
28. **Kruiswijk F, Yuniati L, Magliozzi R, Low TY, Lim R, Bolder R, Mohammed S, Proud CG, Heck AJ, Pagano M, Guardavaccaro D.** 2012. Coupled activation and degradation of eEF2K regulates protein synthesis in response to genotoxic stress. Sci. Signal. **5:**ra40. http://dx.doi.org/10.1126/scisignal.2002718.
29. **Magliozzi R, Low TY, Weijts BG, Cheng T, Spanjaard E, Mohammed S, van Veen A, Ovaa H, de Rooij J, Zwartkruis FJ, Bos JL, de Bruin A, Heck AJ, Guardavaccaro D.** 2013. Control of epithelial cell migration and invasion by the IKKbeta- and CK1alpha-mediated degradation of RAPGEF2. Dev. Cell **27:**574–585. http://dx.doi.org/10.1016/j.devcel.2013.10.023.
30. **Watanabe N, Arai H, Nishihara Y, Taniguchi M, Hunter T, Osada H.** 2004. M-phase kinases induce phospho-dependent ubiquitination of somatic Wee1 by SCFbeta-TrCP. Proc. Natl. Acad. Sci. U. S. A. **101:**4419–4424. http://dx.doi.org/10.1073/pnas.0307700101.
31. **Sakaue-Sawano A, Kurokawa H, Morimura T, Hanyu A, Hama H, Osawa H, Kashiwagi S, Fukami K, Miyata T, Miyoshi H, Imamura T, Ogawa M, Masai H, Miyawaki A.** 2008. Visualizing spatiotemporal dynamics of multicellular cell-cycle progression. Cell **132:**487–498. http://dx.doi.org/10.1016/j.cell.2007.12.033.
32. **Halim VA, Alvarez-Fernandez M, Xu YJ, Aprelia M, van den Toorn HW, Heck AJ, Mohammed S, Medema RH.** 2013. Comparative phosphoproteomic analysis of checkpoint recovery identifies new regulators of the DNA damage response. Sci. Signal. **6:**rs9. http://dx.doi.org/10.1126/scisignal.2003664.
33. **Martínez-Llordella M, Esensten JH, Bailey-Bucktrout SL, Lipsky RH, Marini A, Chen J, Mughal M, Mattson MP, Taub DD, Bluestone JA.** 2013. CD28-inducible transcription factor DEC1 is required for efficient autoreactive CD4+ T cell response. J. Exp. Med. **210:**1603–1619. http://dx.doi.org/10.1084/jem.20122387.